Meson-baryon dynamics in the nucleon-antinucleon system. I. The nucleon-antinucleon interaction

T. Hippchen, J. Haidenbauer, K. Holinde, and V. Mull
Institut für Kernphysik, Forschungszentrum Jülich, D-5170 Jülich, Germany
(Received 27 December 1990)

A model for the nucleon-antinucleon interaction is presented, which is based on meson-baryon dynamics. The elastic part is the G-parity transform of the Bonn NN potential; annihilation is accounted for by microscopic baryon-exchange processes with two-meson intermediate states involving π, ρ, σ, ω, δ, K, and K^*. Results for cross sections and polarization data are compared with a phenomenological treatment of annihilation based on a simple, state- and energy-independent optical potential.

I. INTRODUCTION

Although quantum chromodynamics is believed to be the ultimate theory of strong interactions in terms of the fundamental quarks and gluons, an effective theory based on collective, hadronic degrees of freedom still provides for the most quantitative description of the nucleon-nucleon (NN) interaction at low energies relevant for nuclear physics. The recent Bonn NN potential [1], for example, which beyond traditional one-boson-exchange diagrams also takes into account explicit 2π and $\pi\rho$ exchanges involving (virtual) delta(Δ)-isobar excitations, can reproduce the whole NN phenomenology below pion production threshold.

It is an interesting and important question whether (or to which extent) the same approach also works in the nucleon-antinucleon system, i.e., whether or not a consistent and universal description of both the NN and $N\bar{N}$ interactions is possible within a meson-exchange picture. The $N\bar{N}$ interaction is quite appropriate for exploring the limits of the meson-theoretical description of strong interactions: In contrast to the NN case, the $N\bar{N}$ interaction is attractive in the inner region; therefore the $N\bar{N}$ system should be much more sensitive to effects due to explicit quark-gluon dynamics. The explicit structure of the Bonn potential in terms of meson-baryon couplings (vertices) is especially suited for that purpose since all vertices appearing in the $N\bar{N}$ interaction, in the elastic as well as in the annihilation part, are related to corresponding couplings in the NN interaction. Especially the G-parity transformation, which is used for transforming NN dynamics to the elastic $N\bar{N}$ interaction, can be applied in a clear-cut manner in the particular case of the Bonn potential, since no arbitrary parametrization for the short-ranged NN interaction is introduced. This is essential for a serious test of meson-exchange dynamics at intermediate and small distances. For example, part of the ω exchange, as parametrized in meson-exchange models, might contain contributions due to explicit quark-gluon dynamics, since vector-meson and effective one-gluon exchange have similar characteristics in the NN system [2]. (In fact, the ω coupling constant needed to fit NN (as well as K^+N [3]) data turns out to be much larger than suggested by SU(3) relations.) If, however, these contributions behave differently under G-parity transformation, the resulting elastic $N\bar{N}$ interaction would be much less attractive in the inner region and hopefully lead to noticeable consequences in the description of the $N\bar{N}$ data, as happened in a recent comparative study of the $K^{\pm}N$ system [4]. Such important issues can be investigated only if an *ad hoc* parametrization of the inner part of the elastic $N\bar{N}$ interaction is avoided.

Recently [5], we have shown that a good description of (most) low- and intermediate-energy $N\bar{N}$ data can indeed be achieved when the prescribed state dependence of the G-parity transformed Bonn NN potential [one-boson-exchange version (OBEPT)] is kept completely in the inner region and annihilation is accounted for by a simple phenomenological, energy- and state-independent optical potential with both real and imaginary parts and three adjustable parameters. In the same paper, we have demonstrated that the influence of short-ranged modifications of the elastic $N\bar{N}$ interaction, because of the dominance of annihilation processes, is small but not negligible. Here, we will show that a comparably good fit of the $N\bar{N}$ data can also be achieved by starting from (essentially) the full Bonn potential.

Of course, for a serious test of the meson-exchange concept in the $N\bar{N}$ system and also for a reliable study of specific annihilation channels, it is absolutely essential to treat not only the elastic interaction but also the annihilation processes in the same consistent microscopic framework. Otherwise, discrepancies arising from different treatments of the (short-ranged) elastic $N\bar{N}$ interaction can always be compensated by suitable adjustments in the phenomenological annihilation potential, especially since the $N\bar{N}$ data are not very sensitive to modifications in the elastic part.

Unfortunately, a realistic microscopic treatment of annihilation processes becomes extremely involved (in both the baryon and quark-gluon-exchange approach), for several reasons. For example, annihilation into several (more than two) pions is dominant, and the uncorrelated part of such processes is extremely complicated to evalu-

ate. Furthermore, the inclusion of interactions between the mesons might be important; however, not much is known about them in the relevant energy range.

The present paper represents an admittedly small step in the direction to derive the annihilation processes microscopically in the baryon-exchange framework: We restrict ourselves to two-meson annihilation processes, which is demanded by computational feasibility. Note, however, that, in spite of the high pion multiplicity, this restriction has a lot of justification. In fact, as demonstrated by Vandermeulen [6], the properties of higher-multiplicity channels can be understood, on a phenomenological level, in terms of quasi-two-body ones, replacing clusters of several pions by corresponding resonances.

For consistency, we include all combinations of mesons present in the elastic $N\bar{N}$ interaction (and therefore in the full Bonn NN potential [1]), i.e., π, ρ, σ', ω, and δ. Note that the σ' (with a mass of 550 MeV) is not a real particle but represents a simple effective description of correlated 2π exchange processes. In addition, we take into account annihilation processes into the strange mesons K and K^*, quite in analogy to our hyperon-nucleon interaction [7]. All coupling constants have been taken correspondingly from Refs. [1,7]. At this stage, we have not considered any interaction between the two mesons.

Already at this point, one has to realize the following: Although we treat various two-meson annihilation channels explicitly, these account for at most 30% of the total observed annihilation. For example, annihilation into higher mesons (f_2,a_2) is so far not included. Therefore, in order to reproduce the empirical annihilation cross section, the channels not treated explicitly must be parametrized into those included. This could be done by suitably modifying coupling constants and/or form-factor parameters at the annihilation vertices. We decided to keep the coupling constants the same, and to put the required modification completely into the form factors.

Thus, the whole annihilation is parametrized using the strong spin, isospin, as well as energy dependence predicted by two-meson annihilation. Such a model is the other extreme compared to our phenomenological annihilation model, in which these dependencies are totally suppressed.

The paper is organized as follows: In the next section, we first outline the general scheme and then describe our $N\bar{N}$ interaction model. In Sec. III, we present and discuss the results and compare them with $N\bar{N}$ experiments [8–31]. Finally, Sec. IV contains a short summary.

II. THE $N\bar{N}$ INTERACTION MODEL

A. The general scheme

The construction of the $N\bar{N}$ interaction in the meson-exchange framework goes along the same lines used in the derivation of the Bonn NN potential [1]. Therefore, we start again from a field-theoretical Hamiltonian written as the sum of a free Hamiltonian H_0 and an interaction term W,

$$H = H_0 + W \ . \tag{2.1}$$

Compared to Ref. [1], H_0, in addition to baryon and meson states, now includes also antibaryons as well as antimesons. Correspondingly the interaction term W has now to be generalized to

$$W = \sum_{\alpha\beta\gamma} ({}^1W_{\alpha\beta\gamma} a^\dagger_\alpha a_\beta b_\gamma + {}^2W_{\alpha\beta\gamma} \bar{a}^\dagger_\alpha \bar{a}_\beta b_\gamma + {}^3W_{\alpha\beta\gamma} a^\dagger_\alpha \bar{a}^\dagger_\beta b_\gamma + {}^4W_{\alpha\beta\gamma} \bar{a}_\alpha a_\beta b_\gamma) + \text{H.c.} + (b_\gamma \to \bar{b}_\gamma) \ . \tag{2.2}$$

Here a_α ($\bar{a}_\alpha$) denotes the baryon (antibaryon) annihilation operator; b_γ ($\bar{b}_\gamma$) stands for the corresponding meson (antimeson) operator. The sum goes over all quantum numbers which specify the state completely, i.e., momentum, spin, isospin, and kind of particle.

The various terms are pictorially described in Fig. 1. The first term is the basis of the Bonn potential; the second term emerges in the baryon-antibaryon interaction and is related to the first one by G-parity arguments; the third term builds up the annihilation into mesons. W is obtained in a straightforward way from fundamental interaction Lagrangians $\mathcal{L}$; see Appendix A.

For consistency, we will restrict ourselves to baryons which have been included in the Bonn potential and its extension to the hyperon-nucleon case [7], i.e., N,Λ,Σ (spin $\frac{1}{2}$) and Δ and Y^* (spin $\frac{3}{2}$). Furthermore, as in Refs. [1] and [7], we will not consider vertices involving two spin-$\frac{3}{2}$ baryons.

Based on this field-theoretical Hamiltonian, Eq. (2.1), the scattering matrix T, related to the standard S matrix by

$$\langle f|S|i\rangle = \langle f|i\rangle - 2\pi i \delta(E_f - E_i)\langle f|T|i\rangle \ , \tag{2.3}$$

is given in time-ordered perturbation theory as

$$\langle f|T(Z)|i\rangle = \left\langle f \left| W \left[\sum_{j=0}^{\infty} [G_0(Z+i\varepsilon)W]^j \right] \right| i \right\rangle \ , \tag{2.4}$$

where

$$G_0(Z+i\varepsilon) = \frac{1}{Z - H_0 + i\varepsilon} \tag{2.5}$$

is the free Green's function of the particles in intermediate states and Z is the starting energy.

In order to make the calculation tractable we will suppress any interaction between baryonic states not in-

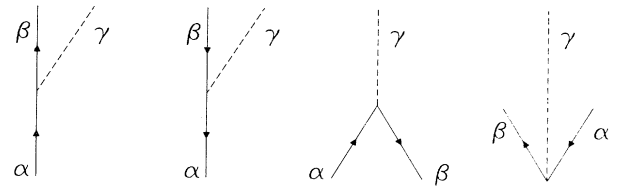

FIG. 1. Various contributions to the vertex function.

volving the $N\bar{N}$ state. Furthermore, at this stage, we will assume that the transition from the baryon-antibaryon sector to the meson sector happens from the $N\bar{N}$ state only.

One then obtains for the $N\bar{N}$ amplitude in channel space

$$\langle N\bar{N}|T|N\bar{N}\rangle = \langle N\bar{N}|V_{\text{eff}}|N\bar{N}\rangle + \langle N\bar{N}|V_{\text{eff}}|N\bar{N}\rangle G_0(N\bar{N})\langle N\bar{N}|T|N\bar{N}\rangle \tag{2.6a}$$

with

$$\langle N\bar{N}|V_{\text{eff}}|N\bar{N}\rangle = \langle N\bar{N}|V|N\bar{N}\rangle + \sum_{B''}\langle N\bar{N}|V|B''\rangle G_0(B'')\langle B''|V|N\bar{N}\rangle + \sum_{M''}\langle N\bar{N}|V|M''\rangle G_0(M'')\langle M''|V|N\bar{N}\rangle , \tag{2.6b}$$

V being of second order in W.

In the c.m. system, both initial and final states are uniquely characterized by the relative momentum and the helicities λ of the particles involved. Equations (2.6) can then be written as

$$\langle \mathbf{q}'\lambda'_N\lambda'_{\bar{N}}|T(Z)|\mathbf{q}\lambda_N\lambda_{\bar{N}}\rangle = \langle \mathbf{q}'\lambda'_N\lambda'_{\bar{N}}|V_{\text{eff}}(Z)|\mathbf{q}\lambda_N\lambda_{\bar{N}}\rangle + \sum_{\lambda''_N\lambda''_{\bar{N}}}\int d^3q''\langle \mathbf{q}'\lambda'_N\lambda'_{\bar{N}}|V_{\text{eff}}(Z)|\mathbf{q}''\lambda''_N\lambda''_{\bar{N}}\rangle \frac{1}{Z-2E_{q''}+i\varepsilon} \times \langle \mathbf{q}''\lambda''_N\lambda''_{\bar{N}}|T(Z)|\mathbf{q}\lambda_N\lambda_{\bar{N}}\rangle , \tag{2.7a}$$

$$\langle \mathbf{q}'\lambda'_N\lambda'_{\bar{N}}|V_{\text{eff}}(Z)|\mathbf{q}\lambda_N\lambda_{\bar{N}}\rangle = \langle \mathbf{q}'\lambda'_N\lambda'_{\bar{N}}|V(Z)|\mathbf{q}\lambda_N\lambda_{\bar{N}}\rangle + \sum_{B''}\sum_{\lambda''_B\lambda''_{\bar{B}}}\int d^3q''\langle \mathbf{q}'\lambda'_N\lambda'_{\bar{N}}|V(Z)|\mathbf{q}''\lambda''_B\lambda''_{\bar{B}}\rangle \frac{1}{Z-E^B_{q''}-E^{\bar{B}}_{q''}+i\varepsilon}\langle \mathbf{q}''\lambda''_B\lambda''_{\bar{B}}|V(Z)|\mathbf{q}\lambda_N\lambda_{\bar{N}}\rangle + \sum_{M''}\sum_{\lambda''_i\lambda''_j}\int d^3k''\langle \mathbf{q}'\lambda'_N\lambda'_{\bar{N}}|V(Z)|\mathbf{k}''\lambda''_i\lambda''_j\rangle \frac{1}{Z-\omega^i_{k''}-\omega^j_{k''}+i\varepsilon} \times \langle \mathbf{k}''\lambda''_i\lambda''_j|V(Z)|\mathbf{q}\lambda_N\lambda_{\bar{N}}\rangle . \tag{2.7b}$$

The above equations are solved numerically, after a straightforward partial-wave expansion.

B. Model for the $N\bar{N}$ potential $V_{\text{eff}}(Z)$

The solution of Eqs. (2.7) requires the knowledge of the $N\bar{N}$ pseudopotential, $\langle N\bar{N}|V_{\text{eff}}(Z)|N\bar{N}\rangle$. Its construction proceeds in two steps: First, we will deal with the elastic $N\bar{N}$ interaction, i.e., with processes which, in the considered low-energy range, do not involve any real transition into another channel. Afterwards, we will derive the annihilation part, which, in our model, consists of transitions to two-meson channels only.

1. The elastic part

The elastic part of our $N\bar{N}$ interaction is essentially obtained by a G-parity transformation of corresponding diagrams in the (full) Bonn NN potential. This model contains, apart from simple one-boson exchange, uncorrelated 2π as well as $\pi\rho$ exchange box and crossed-box processes explicitly, involving NN, $N\Delta$, and $\Delta\Delta$ intermediate states. Correlated 2π exchange processes are parametrized in terms of single σ' exchange, having thus well-defined G parity. In contrast, σ_{OBE} generally used in simple one-boson-exchange NN potentials does not have a well-defined G parity since in practice it accounts for effects arising not only from 2π but also from $\pi\rho$ exchange. This leads to uncertainties in the corresponding $N\bar{N}$ interaction not only in case of NN OBE models, but also if the original, full Bonn potential is chosen as a starting point since it contains $\pi\sigma_{\text{OBE}}$ processes; see Ref. [1]. That is the reason why, in actual calculations, we start from a slightly modified version given also in Ref. [1], in which $\pi\sigma_{\text{OBE}}$ together with $\pi\omega$-exchange processes are omitted, canceling each other anyhow to a large extent. After a slight readjustment of parameters (cf. Table 9 in Ref. [1]) this model provides likewise a good description of the empirical NN data. (In fact, almost identical results for $N\bar{N}$ scattering have been obtained if the original Bonn potential is used, assigning σ_{OBE} a positive G parity.) Some examples of diagrams included in our elastic $N\bar{N}$ interaction are shown in Fig. 2.

In principle, for consistency, one should also consider two additional classes of diagrams; namely, one-boson-exchange diagrams in the s channel [Fig. 3(a)] and processes containing a hyperon-antihyperon pair in intermediate states [Fig. 3(b)]. Both groups contribute to the elastic $N\bar{N}$ interaction, for different reasons: First, due to energy and momentum conservation, the intermediate-state meson in Fig. 3(a) can never become real. Second,

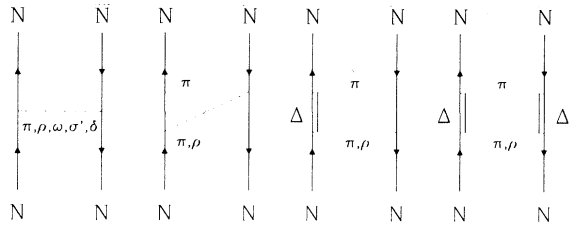

FIG. 2. Some processes contained in our elastic $N\bar{N}$ interaction.

the initial-state energy considered in this work is well below the $\Lambda\bar{\Lambda}$ threshold. It has been checked [32], however, that both contributions have a negligibly small effect on all $N\bar{N}$ data considered.

2. The annihilation part

Our model for the annihilation potential consists of all iterative processes with two-meson intermediate states. (Processes of stretched-box type are comparatively small and are therefore neglected.) We include any combination of $\pi,\sigma',\delta,\rho,\omega$ as well as K,K^* (together with their antiparticles). In consistency with the Bonn NN model [1], the nonstrange mesons are generated not only by nucleon, but also, in case of π and ρ, by Δ exchange; the processes involving strange mesons are likewise generated by Λ, Σ and also Y^* exchange, following our hyperon-nucleon model [7]. For one specific time ordering, the processes included are pictorially described in Fig. 4. In general, there exist 16 different time orderings. For obvious reasons, this number is reduced by half if (i) the intermediate mesons are equal, or (ii) strange mesons are involved. For the general case, all time orderings can be generated by four time orderings of suitably defined transition potentials $\langle M_i M_j|V|N\bar{N}\rangle$. The actual expressions are given in Appendix A.

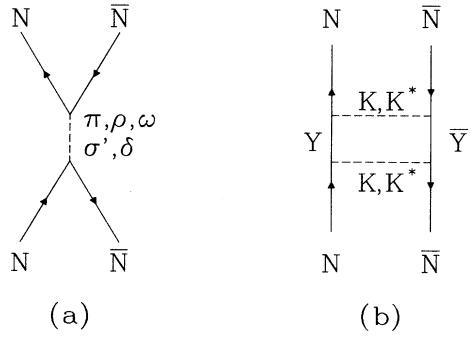

FIG. 3. Additional contributions to the elastic $N\bar{N}$ interaction having negligible effect on $N\bar{N}$ observables: (a) s-channel OBE diagrams, (b) processes with hyperon-antihyperons in intermediate states.

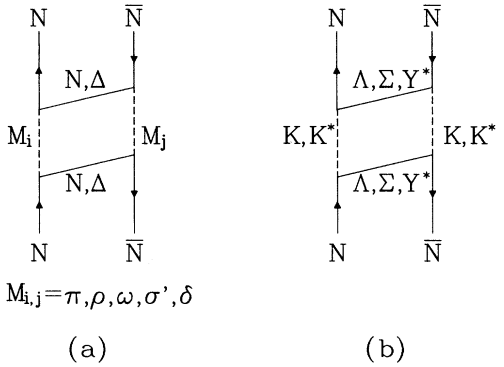

FIG. 4. Processes included in our microscopic annihilation model: (a) nonstrange mesons, (b) strange mesons.

3. Partial-wave expansion, selection rules

For a numerical solution of Eqs. (2.7) we need the partial-wave-projected matrix elements of V_{eff}. We restrict ourselves to the transition potentials into two mesons (the others can be obtained from Ref. [1]). They are defined through the expansion

$$\langle \mathbf{k}\lambda_i\lambda_j|V(Z)|\mathbf{q}\lambda_N\lambda_{\bar{N}}\rangle = \frac{1}{4\pi}\sum_J (2J+1)\, d^J_{\lambda\lambda'}(\cos\theta) \times \langle \lambda_i\lambda_j|V^J(k,q,Z)|\lambda_N\lambda_{\bar{N}}\rangle , \tag{2.8}$$

with $\lambda=\lambda_N-\lambda_{\bar{N}}$ and $\lambda'=\lambda_i-\lambda_j$; $d^J_{\lambda,\lambda'}$ are the well-known reduced rotation matrices [33]. Equation (2.8) can be inverted to give

$$\langle \lambda_i\lambda_j|V^J(k,q,Z)|\lambda_N\lambda_{\bar{N}}\rangle = 2\pi\int_{-1}^{+1} d\cos\theta\, d^J_{\lambda\lambda'}(\cos\theta)\,\langle \mathbf{k}\lambda_i\lambda_j|V(Z)|\mathbf{q}\lambda_N\lambda_{\bar{N}}\rangle . \tag{2.9}$$

Due to parity conservation, only half of them are independent since

$$\langle \lambda_i\lambda_j|V^J(k,q,Z)|\lambda_N\lambda_{\bar{N}}\rangle = P_iP_j(-1)^{S_i+S_j}\langle -\lambda_i-\lambda_j|V^J(k,q,Z)|-\lambda_N-\lambda_{\bar{N}}\rangle , \tag{2.10}$$

where P_i denotes the intrinsic parity of meson i and S_i the corresponding spin. In order to take into account the strong selection rules for the process $N\bar{N}\to M_iM_j$ leading to restrictions for the angular momenta, isospins, and spins, we now have to transform the potentials into the JLS basis,

$$\langle JML'S'|V^J(k,q,Z)|JMLS\rangle = \sum_{\lambda_i\lambda_j\lambda_N\lambda_{\bar{N}}} \langle JML'S'|JM\lambda_i\lambda_j\rangle \times\langle\lambda_i\lambda_j|V^J(k,q,Z)|\lambda_N\lambda_{\bar{N}}\rangle \times\langle JM\lambda_N\lambda_{\bar{N}}|JMLS\rangle , \quad (2.11)$$

with

$$\langle JMLS|JM\lambda_1\lambda_2\rangle = \left[\frac{2L+1}{2J+1}\right]^{1/2}\langle L0S\lambda|J\lambda\rangle\langle S_1\lambda_1 S_2-\lambda_2|S\lambda\rangle . \quad (2.12)$$

The selection rules originate from the conservation of total angular momentum J, isospin I, parity P, and G-parity G in the transition process. One has

$$(-1)^{L+S+I}=\begin{cases} G_iG_j & \text{if both mesons are} \\ & \text{eigenstates of } G , \\ (-1)^{L'+S'+I} & \text{otherwise } (K,K^*) , \end{cases}$$
$$(-1)^{L+1}=P_iP_j(-1)^{L'} , \quad (2.13)$$

with L the relative angular momentum and S the total spin of the two-body system. The primed quantities refer to the two-meson system, the unprimed quantities to the $N\bar{N}$ system.

4. Form factors

A convenient way to take into account effects from the extended hadron structure is by means of form factors supplemented to the pointlike vertex functions deduced from the fundamental Lagrangians. There are two distinct physical phenomena related to this extension. First each "bare" hadron is surrounded by a virtual meson cloud leading to so-called vertex corrections. In principle, such corrections can be evaluated in the meson-exchange framework, although actual calculations become extremely difficult. In addition, even the bare hadrons have an extension originating from their quark-gluon structure, which is completely determined by QCD. However, because of the enormous complexity of QCD in the low-energy regime, their reliable determination is not possible at present and in the foreseeable future. The form factors are meant to take into account both effects, suppressing the meson-exchange contributions for high momentum transfers. Although they depend in general on all three four-momenta involved at the vertex, they are usually parametrized in a simple form depending only on the four-momentum of that particle which is exchanged in the corresponding potentials. Thus, the off-shell dependence appearing in higher iterations is ignored. Furthermore, in the conventional monopole form, the dependence on the zeroth component is likewise suppressed, i.e.,

$$F(\mathbf{p}_\delta)=\left[\frac{\Lambda_\alpha^2-m_\delta^2}{\Lambda_\alpha^2+\mathbf{p}_\delta^2}\right]^{n_\alpha} . \quad (2.14)$$

Such a parametrization is used in the Bonn potential [1] at the NN and $N\Delta$ vertices with $n_\alpha=1$, apart from $n_\alpha=2$ for the $N\Delta\rho$ vertex. The same choice has been made at the strange vertices in our hyperon-nucleon (YN) model [7]. All cutoff masses Λ_α have been determined by a fit to the low-energy NN and YN data.

In our elastic $N\bar{N}$ interaction, baryon-baryon vertices are the same as in our NN model; furthermore, antibaryon-antibaryon vertices are related by G-parity arguments to corresponding baryon-baryon couplings. Therefore, we use for both types of couplings the same monopole form factor with precisely the same values for Λ_α determined already by our NN studies [1], which means that the whole elastic $N\bar{N}$ interaction is completely fixed, i.e., no arbitrary additional cutoff procedure is applied when going from the NN to the $N\bar{N}$ system.

Although, for consistency, the same particles are involved in our microscopic annihilation model as in the elastic part, form factors at annihilation vertices, now accounting for the off-shell behavior of the exchanged baryon, should be taken as independent from corresponding form factors occurring in the elastic interaction, in which the exchanged meson is the essential off-shell particle.

As pointed out already in the Introduction, such an independent treatment is anyhow required at the present stage in order to (roughly) account for those channels not explicitly included. For that purpose, a convenient parametrization turns out to be

$$F(p_\delta)=\left[\frac{\Lambda_\alpha^4+m_\delta^4}{\Lambda_\alpha^4+(p_\delta^2)^2}\right]^{n_\alpha} . \quad (2.15)$$

Although normalized at the exchanged baryon's pole, this form factor is, with values for $\Lambda_\alpha\sim 1.5$ GeV (see results below), considerably larger than 1 in the physical region ($p_\delta^2\leq 0$), especially if $n_\alpha=2$ is used in Eq. (2.15), as it is required for convergence reasons at the $N\Delta\rho$ and NY^*K^* vertices.

5. Phenomenological treatment of annihilation

Our microscopic annihilation model implies a well-defined energy—as well as state—dependence, the latter being very strong due to definite selection rules valid for two-meson annihilation processes [see Eq. (2.13)]. In view of the foregoing discussion the resulting state dependence in our model is probably too extreme since annihilation processes in three or more mesons, now globally taken into account by appropriate form factors, do not fulfill such strict selection rules. This is one of the reasons why we alternatively described (as in Ref. [5]) the annihilation in terms of a state- and energy-independent, simple optical potential of Gaussian form, i.e.,

$$V_{\rm opt}(r)=(U_0+iW_0)e^{-r^2/2r_0^2} . \quad (2.16)$$

Evidently, $V_{\rm opt}$ should contain both a real and imaginary part since it is meant to parametrize terms from second iterations of annihilation processes containing likewise a real and imaginary part.

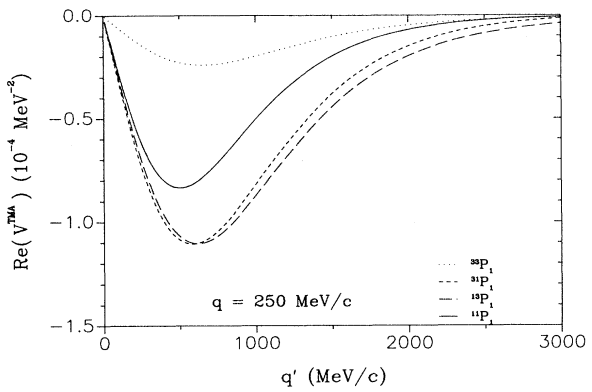

FIG. 5. Real part of the sum of all two-meson annihilation diagrams contributing to $V_{\rm eff}(q,q',Z)$ in the partial waves $^{11}P_1$, $^{31}P_1$, $^{13}P_1$, and $^{33}P_1$ as a function of q'. q and Z are set to 250 MeV.

III. RESULTS AND DISCUSSION

In the meson-exchange framework, annihilation into mesons proceeds via baryon exchange. In spite of the small Compton wavelength (~ 0.1 fm) our resulting annihilation interaction turns out to be very strong (for S waves, about 100 times larger than the elastic part) and still contributes sizably at 1 fm with both an imaginary and a real part. Correspondingly, the $N\bar{N}$ wave function is so much suppressed in the inner region that the annihilation probability peaks at around 1 fm (see Ref. [34]) in agreement with semiempirical findings [35]. Thus baryon-exchange models cannot be rule out just on ground of range arguments referring to the Compton wavelength. In contrast to the phenomenological annihilation potential, Eq. (2.16), the microscopic model has a prescribed energy and state dependence, arising from the vertex structure, the baryon and meson propagators, and strong selection rules. The state dependence is exemplified in Fig. 5 where we show the real part of the sum of all meson annihilation diagrams contributing to $V_{\rm eff}(Z)$ [see Eq. (2.7b)] in P waves with $J=1$. (Cutoff parameters have been chosen as in model C, to be discussed below.) Evidently there are sizable differences whereas the phenomenological annihilation model leads to identical results in all these states.

Our construction of a microscopic $N\bar{N}$ interaction model proceeds in two steps. First (model B), we only consider nonstrange particles in the annihilation part [Fig. 4(a)]; in the next step (model C), we include also hyperon (Λ, Σ, Y^*) exchange for annihilation [Fig. 4(b)]. In both cases, the elastic part consists of the G-parity transform of the (modified) full Bonn potential.

The only free parameters are the cutoff masses Λ_α [see Eq. (2.15)] at the annihilation vertices. The values given in Table I have been chosen in order to obtain a satisfactory description of integrated $p\bar{p}$ elastic and total cross sections, for momenta $p_{\rm lab} \leq 800$ MeV/c. (It was not possible to obtain the charge-exchange cross section in the same time; see below.) The results are most sensitive to variations at the $N\Delta\rho$ and NY^*K^* vertices.

Alternatively, we have parametrized the whole annihilation by the phenomenological optical potential Eq. (2.16), while keeping the elastic part the same [A(BOX)]. Now, with a suitable choice of the three optical potential parameters, it was possible to get a quantitative description of all integrated $N\bar{N}$ cross sections. The resulting values are given in Table II [A(BOX)], together with corresponding values (A(OBE), determined in Ref. [5]), based on a simple OBE parametrization for the elastic part (OBEPT of Ref. [1]). Both the (modified) full Bonn potential and OBEPT are essentially equivalent in the NN system, i.e., lead to descriptions of low-energy NN data of comparable quality. In the $N\bar{N}$ system, however, they are rather different, at least in the inner region, for the following reason: The full Bonn model contains not only (attractive) 2π ($G=+1$) but also $\pi\rho$ ($G=-1$) contributions (repulsive in the NN, but attractive in the $N\bar{N}$ system). Thus, the sum of $2\pi+\pi\rho$ contributions is much more attractive in the $N\bar{N}$ than in the NN system. On the other hand, in a one-boson-exchange model like OBEPT, this sum (plus correlated 2π exchange) is effectively replaced by $\sigma_{\rm OBE}$ exchange. The usual assumption of positive G parity for $\sigma_{\rm OBE}$ then implies the same attraction in the NN and $N\bar{N}$ system.

Indeed, U_0 is required to be more attractive for A(OBE) than in case of A(BOX) since the elastic $N\bar{N}$ interaction is correspondingly less attractive. Although W_0 differs by a factor of 3, both imaginary parts roughly agree at $r \approx 1$ fm (because of the different range parameter r_0), yielding values around 100 MeV. As pointed out already by Dover and Richard [36] and confirmed by our group [34], this feature is essential in order to obtain an overall agreement with the data. The actual combination of parameter values is provided by a fine tuning of the fit only. Finally, we would like to stress that the real part of the annihilation potential is likewise non-negligible at 1 fm, in complete consistency with the microscopic annihilation model.

TABLE I. Form-factor parameters [Eq. (2.15)] at the annihilation vertices, for models B and C.

Vertex	$NN\pi$	$NN\sigma'$	$NN\delta$	$NN\omega$	$NN\rho$	$N\Delta\pi$	$N\Delta\rho$	
Λ_α (GeV)	1.6	1.5	1.5	1.3	1.6	1.5	1.725	C
	1.2	1.5	1.5	1.5	1.8	1.275	1.475	B
Vertex	$N\Lambda K$	$N\Sigma K$	$N\Lambda K^*$	$N\Sigma K^*$	NY^*K	NY^*K^*		
Λ_α (GeV)	1.5	1.5	1.6	1.5	1.5	1.445		C

TABLE II. Parameters of the phenomenological optical potential [Eq. (2.16)] in the models A(BOX) and A(OBE).

	A(BOX)	A(OBE)
U_0	−629 MeV	−1260 MeV
W_0	−4567 MeV	−1575 MeV
r_0	0.36 fm	0.40 fm

Although, as discussed before, there are considerable differences in the employed elastic $N\bar{N}$ interactions, these have only a small influence on the $N\bar{N}$ results, even for polarization observables. This has been demonstrated [5] by comparing the predictions of model A(OBE) with those originating from replacing the elastic OBE interaction by an extended model including box diagrams [it differed from A(BOX) by suppressing noniterative diagrams], but keeping the optical potential parameter values the same as in A(OBE).

Figure 6 shows the resulting total and integrated elastic cross sections calculated for the models B and C together with the results from A(BOX) as well as A(OBE). Obviously, the microscopic models can reproduce the experimental data quite well; the description of the data is of the same quality as obtained with the phenomenological models A(BOX) and A(OBE) and better than the ones obtained from present annihilation models based on quark-gluon exchange mechanisms [37]. It is instructive to investigate which partial waves give the main contributions to the total cross section. While in the NN case more than 90% of the low-energy cross section results from S waves, P waves are now much more important. This is demonstrated in Fig. 7 for models A(BOX) and C. Already at low energies P waves play a considerable role; for $p_{\rm lab} \geq 250$ MeV/c they even exceed the S-wave contribution. In case of model C and at $p_{\rm lab} = 310$ MeV/c, we have 35% S waves, 55% P waves, and 10% D waves. Note that the microscopic (C) as well as the phenomenological (A) descriptions of annihilation, though having completely different characteristics, lead to very similar results.

In contrast to the phenomenological models A, the microscopic annihilation models B and C cannot reproduce the charge-exchange cross section. In particular, for low energies the predictions by far exceed the empirical data. At higher energies, model C is nearer to the data than the restricted model B. The reason for the failure of the microscopic annihilation models lies in their isospin dependence, which is much too strong. Indeed, if we just take the isospin average of the annihilation potential in both isospin channels, all integrated cross sections can be

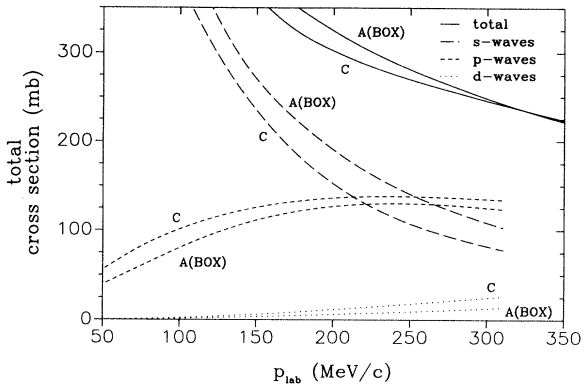

FIG. 7. S-, P-, and D-wave contributions to the total cross sections of our models A(BOX) and C.

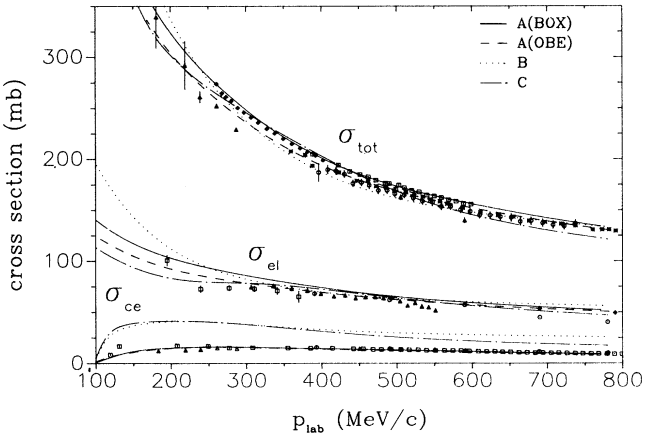

FIG. 6. $\bar{p}p$ total, integrated elastic, and charge-exchange cross sections for our models A(BOX) (solid), A(OBE) (dashed), B (dotted), and C (dash-dotted). Experimental data are from Refs. [8] (circles), [9] (squares), [10] (triangles), [11] (diamonds), and [12] (asterisks) for the total cross section, from Refs. [13] (squares), [14] (triangles), [15] (diamonds), and [16] (circles) for the elastic cross section, and from Refs. [17] (squares), [18] (circles), and [19] (triangles) for the charge-exchange cross section.

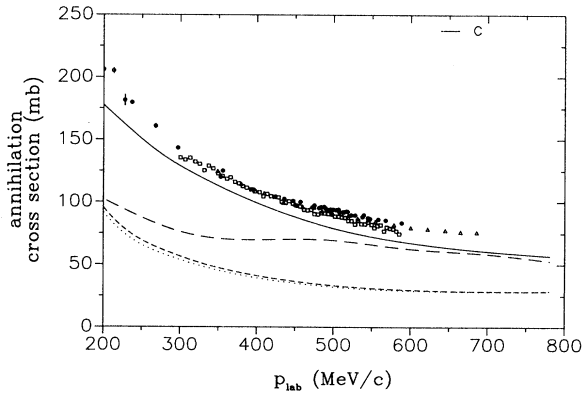

FIG. 8. $\bar{p}p$ annihilation cross section calculated for different ingredients of our microscopic annihilation model. The solid line is the result with the (complete) model C. The long dashed curve is obtained by omitting all diagrams involving strange particles, the short dashed curve after omitting also Δ-exchange diagrams with ρ mesons. The dotted line corresponds to a calculation with N-exchange annihilation diagrams only. Experimental data are from Refs. [12] (triangles), [20] (squares), and [21] (circles).

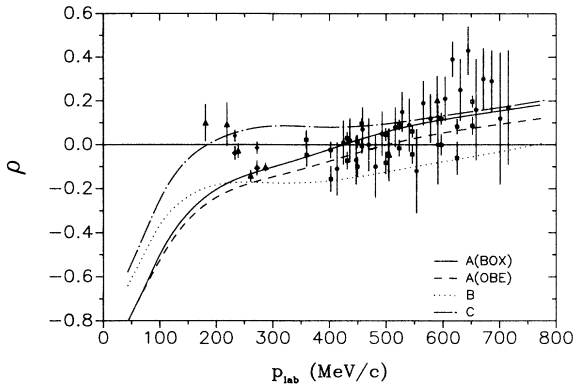

FIG. 9. ρ parameter. Same description of the curves as in Fig. 6. Experimental data are from Refs. [10] (triangles), [22] (circles), [23] (squares), and [24] (diamonds).

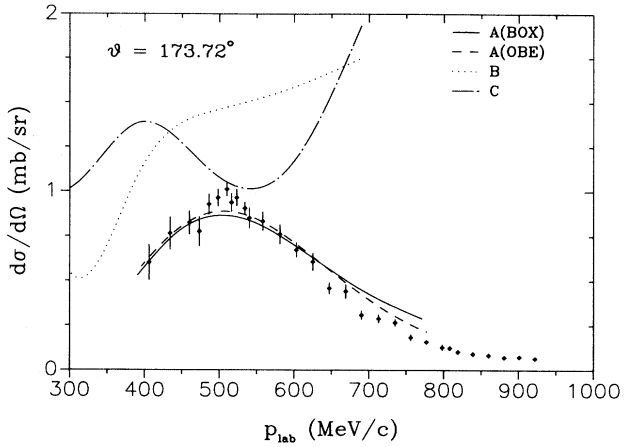

FIG. 11. $p\bar{p}$ backward elastic cross section. Same description of the curves as in Fig. 6. Experimental data are from Ref. [25].

reproduced without any problems, after a suitable parameter readjustment. Alternatively, we have kept the annihilation model with its strong isospin dependence but increased the isospin-independent part of the interaction by doubling the (elastic) ω-exchange contribution. σ_{tot} and σ_{el} could again be reproduced, and σ_{ce} was only 20% too large. (Thus, in our model, σ_{ce} is not completely determined by the longer-range part of the $N\bar{N}$ interaction but can be appreciably changed by modifying the short-range part.) We stress that both modifications are not without physical reasons: First, the isospin dependence in the present annihilation models B and C is probably overestimated since the whole annihilation is de-

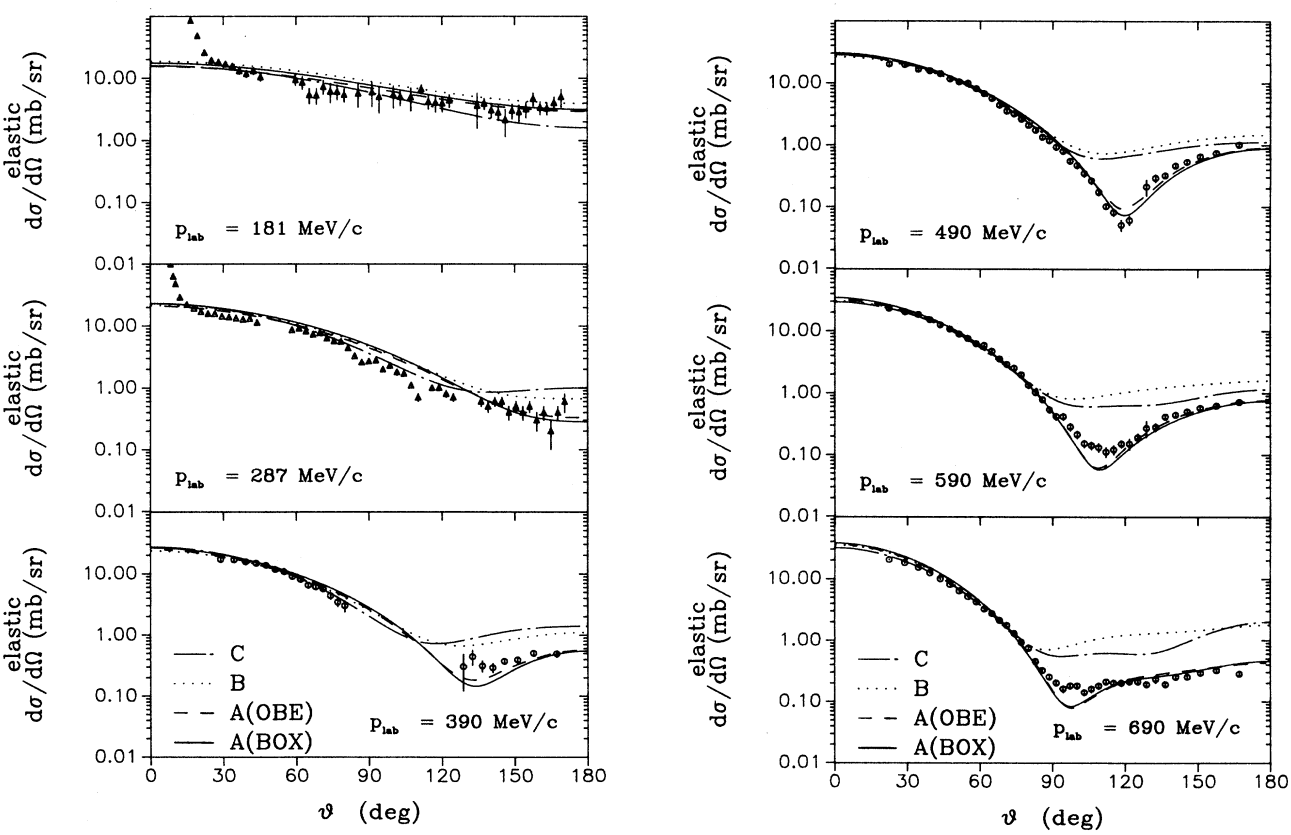

FIG. 10. $\bar{p}p$ elastic differential cross sections. Same description of the curves as in Fig. 6. Experimental data are from Refs. [16] (circles) and [26] (triangles).

scribed in terms of two-meson annihilation processes, which, to a good part, effectively contain three- and higher-order processes; the latter, however, are much less subject to selection rules implying definite isospin dependence. Second, a lot of higher-order processes, which roughly cancel in the NN system and therefore have not been included in the Bonn NN potential as well as in the G-parity transform, all add up in the $N\bar{N}$ system and, if included, would provide more attraction.

Since the charge-exchange cross section is too large, the annihilation cross section is (slightly) too small. Indeed, model B results in 80%, model C in about 90% of the empirical annihilation cross section (see Fig. 8) which represents a definite improvement over present quark-gluon annihilation models yielding only 60% or so. It should be mentioned that we can get easily 100% of the annihilation if we allow the total cross section to become larger. Figure 8 also demonstrates that, because of their vertex structure, vector mesons contribute most significantly to the annihilation, in agreement with empirical findings. For these contributions, Δ and Y^* exchange (with two ρ's and K^*'s, respectively) dominate. Annihilation diagrams with two scalar or pseudoscalar mesons are relatively unimportant, including the transition into two pions via Δ exchange. This is the reason why Moussallam in his first work [38] could not obtain more than 50% of the empirical annihilation; he neither included the $N\Delta\rho$ vertex nor the exchange of hyperons.

Let us now come to our predictions for the ρ parameter, which is the ratio of the real to imaginary part of the forward $p\bar{p} \to p\bar{p}$ amplitude. The results are presented in Fig. 9. Contrary to the phenomenological annihilation models A(BOX) and A(OBE) (and all comparable models in the literature) our meson-theoretic annihilation models based on baryon exchange do provide a shoulder at lower energies as suggested by experiment, while keeping the smooth behavior of the total cross section. The reason for this shoulder lies in the definite energy—and state—dependence together with strong nonlocalities in the annihilation interaction, which appear automatically, i.e., emerge in a very natural way from the underlying theory.

The resulting elastic differential cross sections are shown in Fig. 10, for various laboratory momenta. Note that so far we have not included the Coulomb interaction in the $p\bar{p}$ channel; as expected, its omission leads to some deficiencies for differential cross sections in the forward direction. Obviously, for low energies the microscopic models B and C come up to a comparably good description as the phenomenological model A; with increasing energy, however, the microscopic models show deficiencies in the backward region.

This is clearly borne out by Fig. 11, which shows the

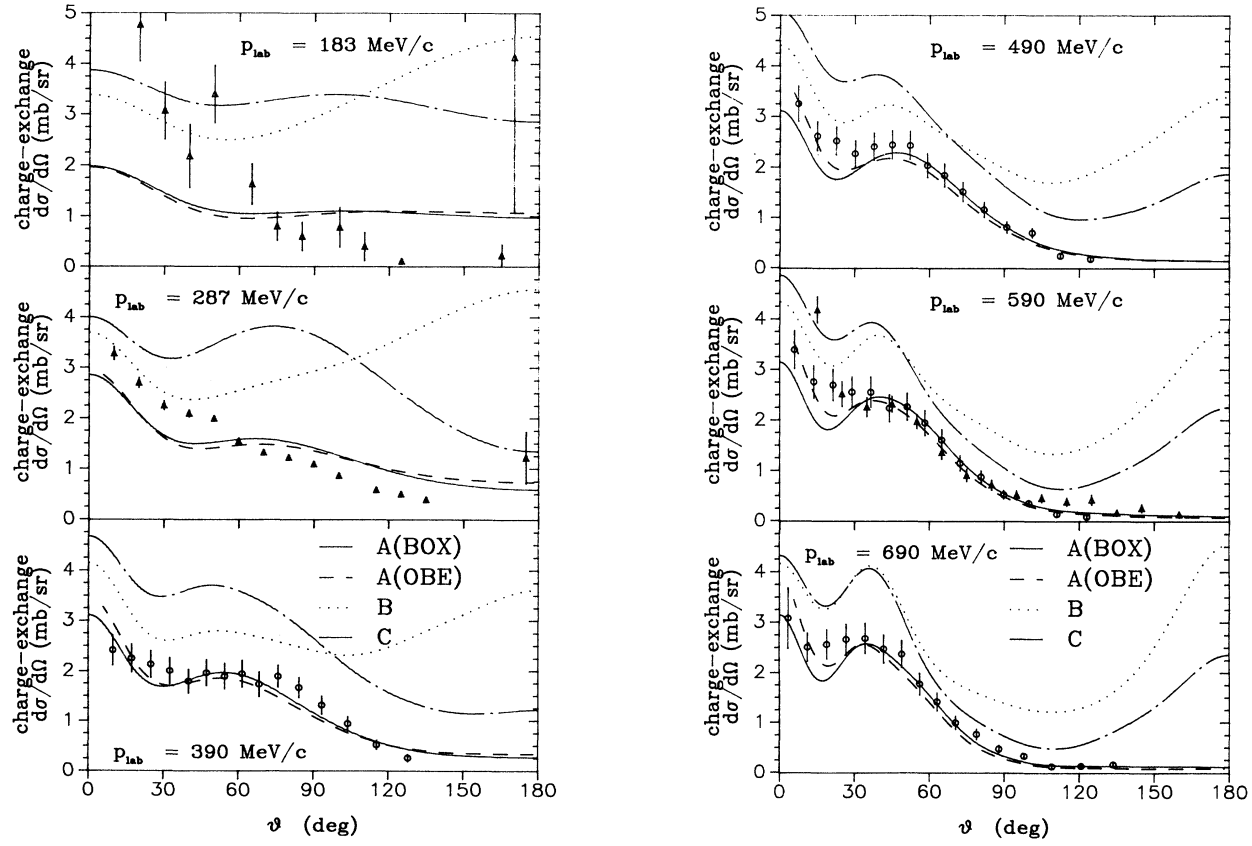

FIG. 12. $p\bar{p}$ charge-exchange differential cross sections. Same description of the curves as in Fig. 6. Experimental data are from Refs. [18] (circles) and [19] (triangles).

backward differential cross section in the elastic $p\bar{p}$ channel. The reproduction of these data does not follow automatically from a good description of integrated cross sections since differential cross sections have their most important contributions for angles smaller than 90°; consequently, the backward region has only a small influence on the (integrated) elastic cross section. Obviously, our phenomenological annihilation models A(BOX), A(OBE) provide good agreement for small and medium energies (with small discrepancies for $p_{\rm lab} > 650$ MeV/c) whereas the microscopic annihilation models show strong deficiencies.

A similar situation occurs for the charge-exchange differential cross sections, see Fig. 12, and for the polarization in the elastic (Fig. 13) and charge-exchange (Fig. 14) channel. The phenomenological models A(BOX), A(OBE) provide a reasonable reproduction of the empirical data whereas the microscopic models fail strongly. Obviously, their spin-isospin structure is not yet correct in the present stage. The remarkable differences in the predictions of models B and C—despite their similar structure—suggest, however, a strong sensitivity of the differential cross sections and polarization data even to small variations in the potential. Thus there is reason to hope that the inclusion of further annihilation channels (e.g., those involving f_2 and a_2 mesons) into our microscopic model (which is currently under way) will improve the situation.

Finally, in Fig. 15 we compare the results for the Wolfenstein parameters D, A, and R. Again, as for the polarizations, there are strong differences, especially at larger angles. It is interesting that the depolarizations predicted by our models B and C are in fair agreement with the few experimental data available while the models with phenomenological annihilation show strong discrepancies. Obviously, these data show the limits of a simple, state- and energy-independent description of the annihilation.

IV. SUMMARY

In this paper we have investigated the nucleon-antinucleon interaction from the meson-exchange point of view, in complete analogy and consistency with former studies of the nucleon-nucleon, hyperon-nucleon, and kaon-nucleon systems performed by the Bonn-Jülich group [1,3,4,7].

The elastic $N\bar{N}$ interaction is obtained by a G-parity transform of the (slightly modified) full Bonn NN potential. Annihilation is accounted for by microscopic

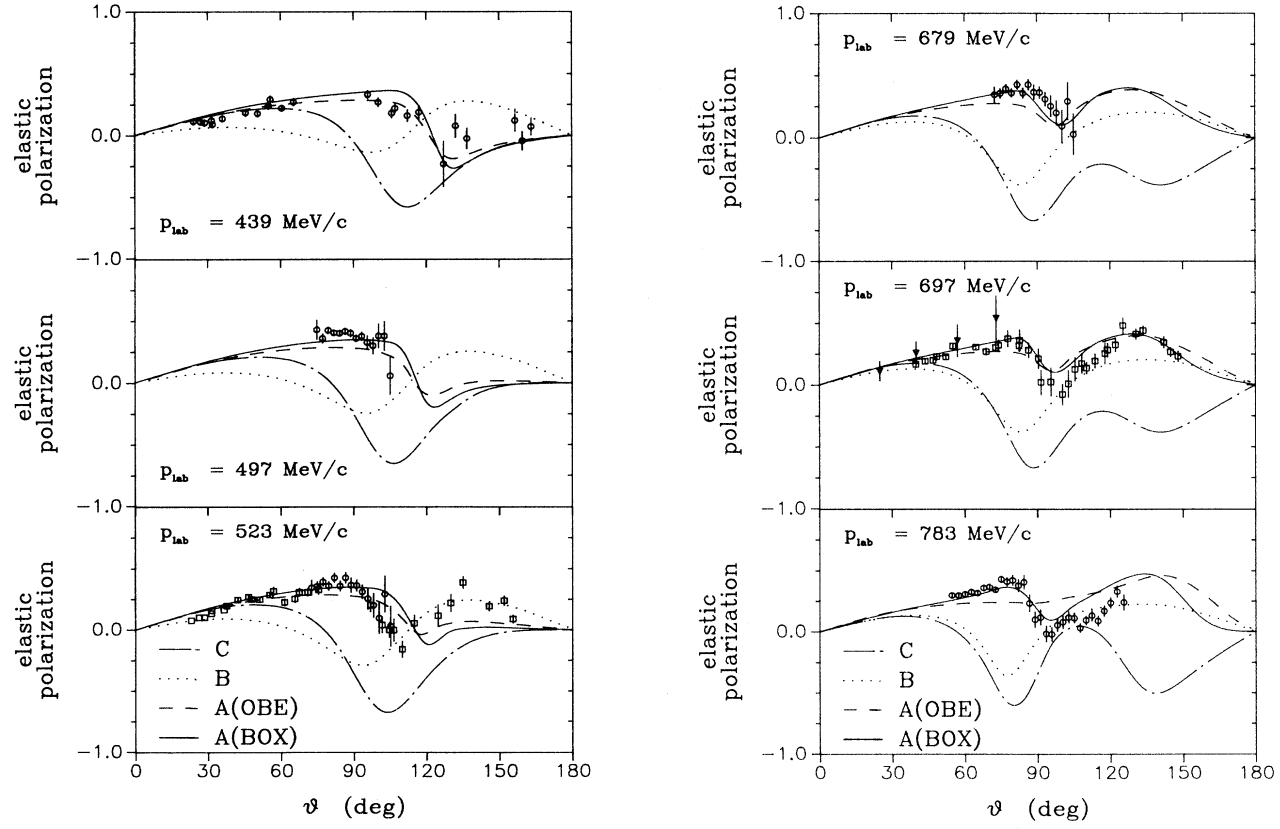

FIG. 13. $\bar{p}p$ elastic polarizations. Same description of the curves as in Fig. 6. Experimental data are from Refs. [27] (triangles), [28] (circles), and [29] (squares).

baryon-exchange processes based on N, Δ, Λ, Σ, and Y^* exchange and involving all combinations of the mesons π, σ', δ, ρ, ω, K, and K^*. Coupling constants at the annihilation vertices have been taken in consistency with the elastic part or with our hyperon-nucleon model [7]; form-factor parameters (cutoff masses), however, have been (and should be) chosen differently for two basic reasons: First, the essential off-shell particle is now the baryon, not the meson as in the elastic part; second, unavoidably at the present stage, our microscopic annihilation model parametrizes a lot of additional processes not treated explicitly in order to roughly reproduce the total empirical annihilation.

Alternatively, we have presented another model A(BOX), which is based on the same G-parity transform but includes in addition a simple phenomenological, state- and energy-independent optical potential.

Open parameters are adjusted to the integrated $N\bar{N}$ cross sections and predictions are made for differential cross sections and spin observables. The phenomenological annihilation models A(BOX) and A(OBE) [5] can reproduce all existing empirical data with the same quality as other comparable $N\bar{N}$ models, such as the Paris [39], Nijmegen [40], and Dover-Richard [41] potentials. Due to the strong isospin dependence of the microscopic annihilation models, the integrated charge-exchange cross section in that case turned out to be considerably too high, which implies that the resulting annihilation cross section is slightly (about 10%) too low. Nevertheless, this represents already a definite improvement compared to quark-gluon models based on rearrangement and annihilation diagrams. In this connection, it was essential to include annihilation processes involving two vector mesons.

There also exist definite deficiencies in spin observables, for the microscopic annihilation models, which

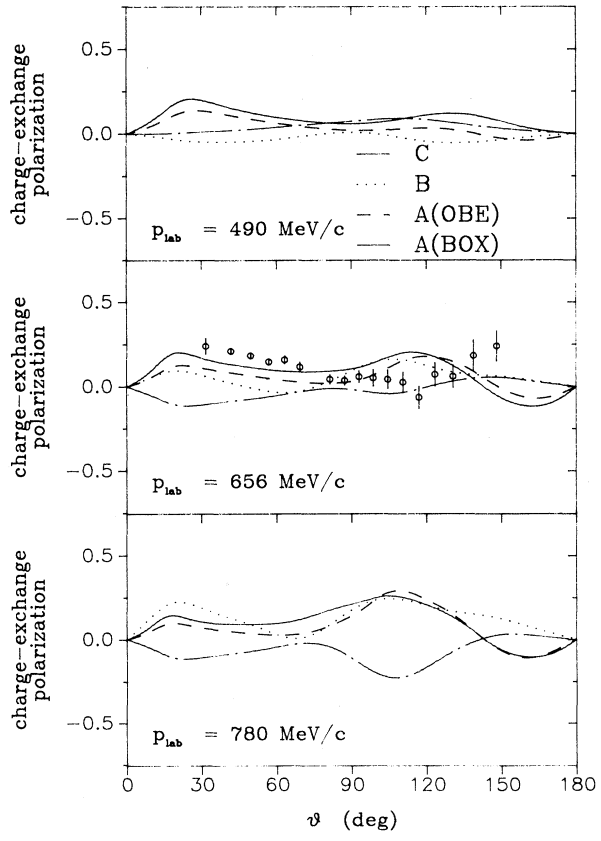

FIG. 14. $\bar{p}p$ charge-exchange polarizations. Same description of the curves as in Fig. 6. Experimental data are from Ref. [30].

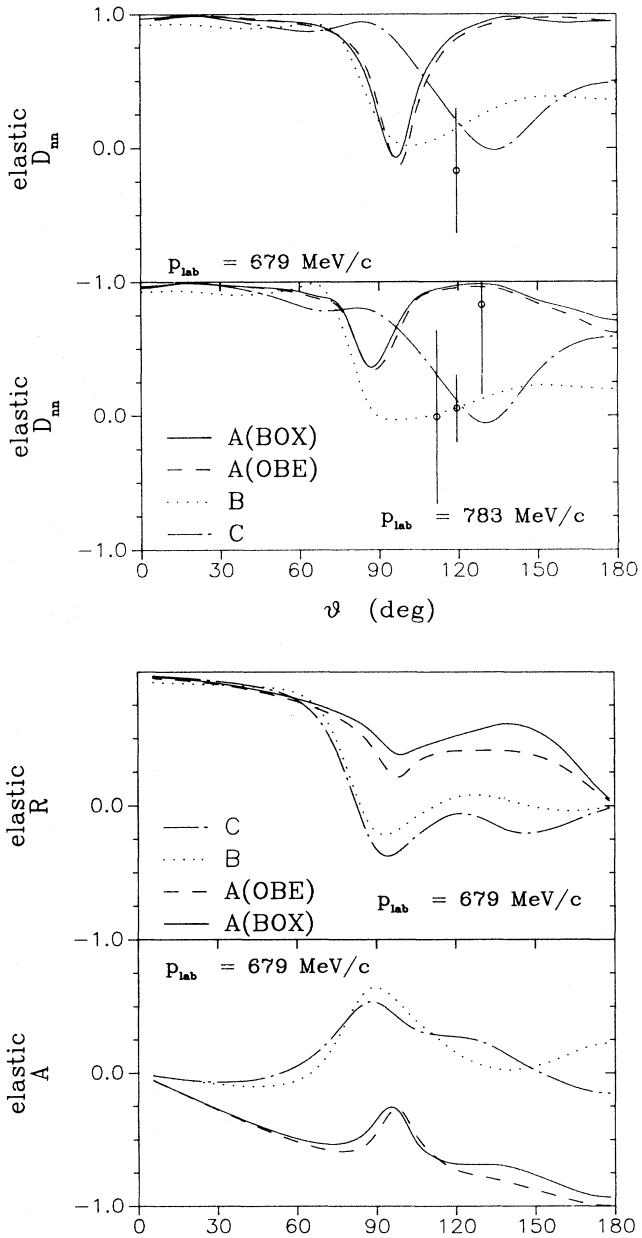

FIG. 15. $\bar{p}p$ elastic spin observables D_{nn}, A, and R. Same description of the curves as in Fig. 6. Experimental data are from Ref. [31].

clearly demonstrate that the resulting spin dependence cannot yet be correct. It was checked that no essential improvement is obtained by varying the available free parameters and still keeping a good description of the integrated total and elastic cross sections.

We stress, however, that the present situation cannot be used as an argument against the baryon-exchange concept in general. As pointed out already in the Introduction, the present calculation should be regarded as a first step only since there is considerable room for improvement. For example, annihilation into (heavier) 1^+ and 2^+ mesons as well as realistic meson-meson interactions should be included, which will surely change the resulting state dependence. Corresponding calculations are presently under way.

We are grateful to Professor J. Speth for his steady interest in this work and for many helpful comments.

APPENDIX A: BARYON-EXCHANGE TRANSITION POTENTIALS

The starting point is the interaction Lagrangians specifying the coupling of the baryons to the various mesons. We have two groups.

(a) Coupling of two spin-$\frac{1}{2}$ baryons with a meson:

Scalar meson 0^+:

$$\mathcal{L}_s=\sqrt{4\pi}g_s\bar{\Psi}_{B'}(x)\Psi_B(x)\Phi^j(x)+\text{H.c.} \tag{A1a}$$

Pseudoscalar meson 0^-:

$$\mathcal{L}_p=\sqrt{4\pi}\frac{f_p}{m_p}\bar{\Psi}_{B'}(x)\gamma^5\gamma^\mu\Psi_B(x)\partial_\mu\Phi^j(x)+\text{H.c.} \tag{A1b}$$

Vector meson 1^-:

$$\mathcal{L}_v=\sqrt{4\pi}g_v\bar{\Psi}_{B'}(x)\gamma^\mu\Psi_B(x)\Phi^j_\mu(x)+\sqrt{4\pi}\frac{f_v}{4m_N}\bar{\Psi}_{B'}(x)\sigma^{\mu\nu}\Psi_B(x)[\partial_\mu\Phi^j_\nu(x)-\partial_\nu\Phi^j_\mu(x)]+\text{H.c.} \tag{A1c}$$

(b) Coupling of a spin-$\frac{1}{2}$ baryon with a spin-$\frac{3}{2}$ baryon and a meson:

Pseudoscalar meson 0^-:

$$\tilde{\mathcal{L}}_p=\sqrt{4\pi}\frac{\tilde{f}_p}{m_p}\bar{\Psi}_{B'}(x)\Psi^\mu_B(x)\partial_\mu\Phi^j(x)+\text{H.c.} \tag{A2a}$$

Vector meson 1^-:

$$\tilde{\mathcal{L}}_v=\sqrt{4\pi}\frac{\tilde{f}_v}{m_v}\bar{\Psi}_{B'}(x)i\gamma^5\gamma^\mu\Psi^\nu_B(x)[\partial_\mu\Phi^j_\nu(x)-\partial_\nu\Phi^j_\mu(x)]+\text{H.c.} \tag{A2b}$$

Here, Ψ_B ($B=N,\Lambda,\Sigma$) are the spin-$\frac{1}{2}$ baryon field operators and Ψ^μ_B ($B=\Delta,Y^*$) the spin-$\frac{3}{2}$ operators; Φ^j are the field operators of meson j. If ingoing and outgoing baryons are different ($B'\neq B$), the Hermitian conjugate has to be added, as indicated in Eqs. (A1) and (A2). Note that these expressions involve only the space-spin part; the isospin dependence can be separated and will be treated later.

With the standard representation of field operators given, e.g., in Ref. [1] and the ansatz for the interaction Hamiltonian

$$W=-\int d^3x\mathcal{L}\ , \tag{A3}$$

the transition potentials, being second order in W,

$$\langle M_iM_j|V|N\bar{N}\rangle=\left\langle M_iM_j\left|\frac{1}{Z-H_0+i\varepsilon}\right|N\bar{N}\right\rangle\ , \tag{A4}$$

can be evaluated in a straightforward way. There are four different contributions, namely, two time orderings together with exchange contributions; see Fig. 16. The latter can simply be taken into account by a factor of 2 in the allowed states.

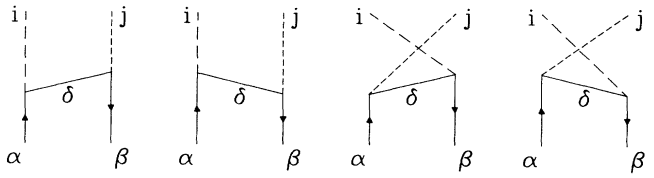

FIG. 16. Four time orderings of the transition potential.

In the case of the exchange of a spin-$\frac{1}{2}$ baryon, the first diagram corresponds to

$$\langle\mathbf{k}\lambda_i\lambda_j|^1U_{ij}|\mathbf{q}\lambda_N\lambda_{\bar{N}}\rangle=\frac{F^i(p_\delta^2)F^j(p_\delta^2)}{4\pi^2}\frac{1}{\sqrt{\omega_k^i\omega_k^j}(Z-\omega_k^i-E_\delta-E_N)}\times\sum_{\lambda_\delta}[\bar{u}(\mathbf{q},\lambda_N)\Gamma^{(i)}u_\delta(\mathbf{p}_\delta,\lambda_\delta)\bar{u}_\delta(\mathbf{p}_\delta,\lambda_\delta)\Gamma^{(j)}v(-\mathbf{q},\lambda_{\bar{N}})]^*\ ; \tag{A5a}$$

the second diagram yields

$$\langle\mathbf{k}\lambda_i\lambda_j|^2U_{ij}|\mathbf{q}\lambda_N\lambda_{\bar{N}}\rangle=\frac{F^i(p'^2_\delta)F^j(p'^2_\delta)}{4\pi^2}\frac{-1}{\sqrt{\omega_k^i\omega_k^j}(Z-E_N-E_\delta-\omega_k^j)}\times\sum_{\lambda_\delta}[\bar{u}(\mathbf{q},\lambda_N)\Gamma^{(i)}v_\delta(-\mathbf{p}_\delta,\lambda_\delta)\bar{v}_\delta(-\mathbf{p}_\delta,\lambda_\delta)\Gamma^{(j)}v(-\mathbf{q},\lambda_{\bar{N}})]^*\ , \tag{A5b}$$

with

$$\Gamma^{(s)}=g_s I_4 ,$$

$$\Gamma^{(p)}=-i\frac{f_p}{m_p}\gamma^5\gamma^\mu k_{j,\mu} , \tag{A6}$$

$$\Gamma^{(v)}=\left[g_v\gamma^\mu+i\frac{f_v}{2m_N}\sigma^{\mu\nu}k_{j,\nu}\right]\varepsilon_\mu(\mathbf{k}_j,\lambda_j) .$$

Here, $p'_\delta\equiv(E_\delta,-\mathbf{p}_\delta)$, $\mathbf{p}_\delta=\mathbf{q}-\mathbf{k}$. Since we will use conventional form factors, which depend only on the momentum of the exchanged particle, we suppress the dependence on the other momenta.

The spin sum over intermediate states can be performed by introducing suitable projection operators

$$\Lambda^+(\mathbf{p}_\delta)=\sum_{\lambda_\delta}u_\delta(\mathbf{p}_\delta,\lambda_\delta)\bar{u}_\delta(\mathbf{p}_\delta,\lambda_\delta)$$
$$=\frac{1}{2E_\delta}(\gamma^0E_\delta-\boldsymbol{\gamma}\cdot\mathbf{p}_\delta+m_\delta I_4) , \tag{A7a}$$

$$\Lambda^-(-\mathbf{p}_\delta)=-\sum_{\lambda_\delta}v_\delta(-\mathbf{p}_\delta,\lambda_\delta)\bar{v}_\delta(-\mathbf{p}_\delta,\lambda_\delta)$$
$$=\frac{1}{2E_\delta}(-\gamma^0E_\delta-\boldsymbol{\gamma}\cdot\mathbf{p}_\delta+m_\delta I_4) . \tag{A7b}$$

In the case of the exchange of a spin-$\frac{3}{2}$ baryon, we have correspondingly

$$\langle\mathbf{k}\lambda_i\lambda_j|^1U_{ij}(Z)|\mathbf{q}\lambda_N\lambda_{\bar{N}}\rangle=\frac{F^i(p_\delta^{\prime\,2})F^j(p_\delta^{\prime\,2})}{4\pi^2}\frac{1}{\sqrt{\omega_k^i\omega_k^j}(Z-\omega_k^i-E_\delta-E_N)}$$
$$\times\sum_{\lambda_\delta}[\bar{u}(\mathbf{q},\lambda_N)\tilde{\Gamma}^{(i)}u_\delta^\mu(\mathbf{p}_\delta,\lambda_\delta)\bar{u}_\delta^\nu(\mathbf{p}_\delta,\lambda_\delta)\tilde{\Gamma}^{(j)}v(-\mathbf{q},\lambda_{\bar{N}})]^* , \tag{A8a}$$

$$\langle\mathbf{k}\lambda_i\lambda_j|^2U_{ij}|\mathbf{q}\lambda_N\lambda_{\bar{N}}\rangle=\frac{F^i(p'^{\,2}_\delta)F^j(p'^{\,2}_\delta)}{4\pi^2}\frac{-1}{\sqrt{\omega_k^i\omega_k^j}(Z-E_N-E_\delta-\omega_k^j)}$$
$$\times\sum_{\lambda_\delta}[\bar{u}(\mathbf{q},\lambda_N)\tilde{\Gamma}^{(i)}v_\delta^\mu(-\mathbf{p}_\delta,\lambda_\delta)\bar{v}_\delta^{\,\nu}(-\mathbf{p}_\delta,\lambda_\delta)\tilde{\Gamma}^{(j)}v(-\mathbf{q},\lambda_{\bar{N}})]^* , \tag{A8b}$$

with

$$\tilde{\Gamma}^{(p)}=-i\frac{\tilde{f}_p}{m_p}k_{j,\mu} ,$$

$$\tilde{\Gamma}^{(v)}=-\frac{\tilde{f}_v}{m_v}\gamma^5\gamma^\nu[k_{j,\nu}\varepsilon_\mu(\mathbf{k}_j,\lambda_j)-k_{j,\mu}\varepsilon_\nu(\mathbf{k}_j,\lambda_j)] . \tag{A9}$$

Here, u_δ^μ (v_δ^μ) denotes the Rarita-Schwinger spinor of the spin-$\frac{3}{2}$ baryon (antibaryon). Corresponding projection operators are not uniquely determined and have ambiguities in the off-shell behavior, which, however, turned out

TABLE III. Isospin factors for $I=0,1$ which multiply corresponding transition potentials in Eqs. (A5) and (A8).

Exchanged baryon	$I=0$	$I=1$
	two isovector mesons	
N	$-\sqrt{6}$	-2
Δ	$-\sqrt{\frac{8}{3}}$	$\frac{2}{3}$
	isovector and isoscalar meson	
N	0	$-\sqrt{2}$
	two isoscalar mesons	
N	$-\sqrt{2}$	0
	two isospin-$\frac{1}{2}$ mesons	
Λ	1	1
Σ, Y^*	3	-1

to have a small effect on our results. We have used

$$P_{+}^{\mu\nu}(\mathbf{p}_\delta)=\sum_{\lambda_\delta} u_\delta^{\mu}(\mathbf{p}_\delta,\lambda_\delta)\bar{u}_\delta^{\nu}(\mathbf{p}_\delta,\lambda_\delta)$$

$$=\Lambda^{+}(\mathbf{p}_\delta)\left[-g^{\mu\nu}+\frac{\gamma^\mu\gamma^\nu}{3}+\frac{2p_\delta^\mu p_\delta^\nu}{3m_\delta^2}-\frac{p_\delta^\mu\gamma^\nu-p_\delta^\nu\gamma^\mu}{3m_\delta}\right] \quad \text{(A10a)}$$

and

$$P_{-}^{\mu\nu}(-\mathbf{p}_\delta)=-\sum_{\lambda_\delta} v_\delta^{\mu}(-\mathbf{p}_\delta,\lambda_\delta)\bar{v}_\delta^{\nu}(-\mathbf{p}_\delta,\lambda_\delta)$$

$$=\Lambda^{-}(-\mathbf{p}_\delta)\left[-g^{\mu\nu}+\frac{\gamma^\mu\gamma^\nu}{3}+\frac{2p_\delta^{\mu'}p_\delta^{\nu'}}{3m_\delta^2}+\frac{p_\delta^{\mu'}\gamma^\nu-p_\delta^{\nu'}\gamma^\mu}{3m_\delta}\right]. \quad \text{(A10b)}$$

The isospin dependence of the transition potentials separates completely from the momentum and spin-dependent part. The corresponding factors, which characterize the dependence of the various processes on the total isospin ($I=0$ or 1) of the initial state, are given in Table III.

[1] R. Machleidt, K. Holinde, and Ch. Elster, Phys. Rep. **149**, 1 (1987).
[2] K. Holinde, Nucl. Phys. **A415**, 477 (1984).
[3] R. Büttgen, K. Holinde, A. Müller-Groeling, J. Speth, and P. Wyborny, Nucl. Phys. **A506**, 586 (1990).
[4] A. Müller-Groeling, K. Holinde, and J. Speth, Nucl. Phys. **A513**, 557 (1990).
[5] T. Hippchen, K. Holinde, and W. Plessas, Phys. Rev. C **39**, 761 (1989).
[6] J. Vandermeulen, Z. Phys. C **37**, 563 (1988).
[7] B. Holzenkamp, K. Holinde, and J. Speth, Nucl. Phys. **A500**, 485 (1989).
[8] K. Nakamura *et al.*, Phys. Rev. D **29**, 349 (1984).
[9] A. S. Clough *et al.*, Phys. Lett. **146B**, 299 (1984).
[10] W. Brückner *et al.*, Phys. Lett. **158B**, 180 (1985).
[11] D. V. Bugg *et al.*, Phys. Lett. B **194**, 563 (1987).
[12] R. P. Hamilton, T. P. Pun, R. D. Tripp, H. Nicholson, and D. M. Lazarus, Phys. Rev. Lett. **44**, 1182 (1980).
[13] D. Spencer and D. N. Edwards, Nucl. Phys. **B19**, 501 (1970).
[14] V. Chaloupka *et al.*, Phys. Lett. **61B**, 487 (1976).
[15] M. Coupland, E. Eisenhandler, W. R. Gibson, P. I. P. Kalmus, and A. Astbury, Phys. Lett. **71B**, 460 (1977).
[16] T. Kageyama, T. Fujii, K. Nakamura, F. Sai, S. Sakamoto, S. Sato, T. Takahashi, T. Tanimori, and S. S. Yamamoto, Phys. Rev. D **35**, 2655 (1987).
[17] R. P. Hamilton, T. P. Pun, R. D. Tripp, H. Nicholson, and D. M. Lazarus, Phys. Rev. Lett. **44**, 1179 (1980).
[18] K. Nakamura, T. Fujii, T. Kageyama, F. Sai, S. Sakamoto, S. Sato, T. Takahashi, T. Tanimori, S. S. Yamamoto, and Y. Takada, Phys. Rev. Lett. **53**, 885 (1984).
[19] W. Brückner *et al.*, Phys. Lett. **169B**, 302 (1986).
[20] T. Brando *et al.*, Phys. Lett. **158B**, 505 (1985).
[21] W. Brückner *et al.*, Z. Phys. A **335**, 217 (1990).
[22] H. Iwasaki *et al.*, Nucl. Phys. **A433**, 580 (1985).
[23] V. Ashford, M. E. Sainio, M. Sakitt, J. Skelly, R. Debbe, W. Fickinger, R. Marino, and D. K. Robinson, Phys. Rev. Lett. **54**, 518 (1985).
[24] L. Linssen *et al.*, Nucl. Phys. **A469**, 726 (1987).
[25] M. Alston-Garnjost, R. P. Hamilton, R. W. Kenney, D. L. Pollard, R. D. Tripp, H. Nicholson, and D. M. Lazarus, Phys. Rev. Lett. **43**, 1901 (1979).
[26] W. Brückner *et al.*, Phys. Lett. **166B**, 113 (1986).
[27] M. Kimura *et al.*, Nuovo Cimento **71A**, 438 (1982).
[28] R. A. Kunne *et al.*, Phys. Lett. B **206**, 557 (1988); R. A. Kunne *et al.*, Nucl. Phys. **B323**, 1 (1989).
[29] R. Bertini *et al.*, Phys. Lett. B **228**, 531 (1989); F. Perrot-Kunne *et al.*, Phys. Lett. B **261**, 188 (1991).
[30] R. Birsa *et al.*, Phys. Lett. B **246**, 267 (1990).
[31] R. A. Kunne, *et al.*, Phys. Lett. B **261**, 191 (1991).
[32] T. Hippchen, Ph.D. thesis, Jül.-Spez. 494, Jülich, 1988.
[33] M. Jacob and G. C. Wick, Ann. Phys. Lett. (N.Y.) **7**, 404 (1959).
[34] J. Haidenbauer, T. Hippchen, K. Holinde, and J. Speth, Z. Phys. A **334**, 467 (1989); J. Haidenbauer, T. Hippchen, and K. Holinde, Nucl. Phys. **A508**, 329c (1990).
[35] T.-A. Shibata *et al.*, Phys. Lett. B **189**, 232 (1987).
[36] C. B. Dover and J. M. Richard, Phys. Rev. C **21**, 1466 (1980).
[37] A. M. Green and J. A. Niskanen, in *Progress in Particle and Nuclear Physics, Vol. 18,* edited by A. Fässler (Pergamon, New York, 1987), p. 93 .
[38] B. Moussallam, Nucl. Phys. **A407**, 413 (1983); **A429**, 429 (1984).
[39] J. Côté, M. Lacombe, B. Loiseau, B. Moussallam, and R. Vinh Mau, Phys. Rev. Lett. **48**, 1319 (1982).
[40] P. H. Timmers, W. A. van der Sanden, and J. J. deSwart, Phys. Rev. D **29**, 1928 (1984).
[41] C. B. Dover and J. M. Richard, Phys. Rev. C **25**, 1952 (1982).